Porous Epoxies by Reaction Induced Phase Separation of Removable Alcohols: Control of Spheroidal Pore Size by Mass Fraction, Cure Temperature, and Reaction Rate

Robert J. Klein,[1]* Mathew C. Celina,[1] Joseph L. Lenhart[1,2]†

[1]*Sandia National Laboratories, Albuquerque, New Mexico 87185*
[2]*US Army Research Laboratory, Aberdeen Proving Ground, Maryland 21005*

Received 17 September 2008; accepted 22 April 2009
DOI 10.1002/app.30702
Published online 6 May 2010 in Wiley InterScience (www.interscience.wiley.com).

ABSTRACT: Porous organic and inorganic materials with both random and controlled microstructures have utility in a variety of fields including catalysis, sensors, separations, optical platforms, tissue engineering, hydrogen storage, micro-electronics, medical diagnostics, as well as other applications. This work highlights a simple and general technique for tuning the pore size in crosslinking polymeric systems by adding a solvent poragen that phase separates during the curing process (reaction induced phase separation). The pore size can be controlled over large length scales ranging from microns to well below 100 nanometers. In this system an amine cured epoxy resin was reacted in the presence of the sacrificial poragen octadecanol, which is removed by vacuum-assisted evaporation once the epoxy components have reacted to form a solid, porous matrix. The importance of the present approach is based on the simplicity of the chemical formulation, the ease by which other epoxide or amine chemistries may be substituted for the two reactive components, and the control of pore size down to the nanometer scale by the addition of a small amount of catalyst. © 2010 Wiley Periodicals, Inc.† J Appl Polym Sci 117: 3300–3307, 2010

Key words: phase separation; reactive processing; sensors; reaction induced phase separation; porous; polymer; epoxy

INTRODUCTION

Precise control of porosity on the micron to nanometer scale is critically important to many polymer applications. Recent examples of applications utilizing porosity for improved properties are silica aerogels,[1] chemical sensors,[2–4] battery electrolytes and electrodes,[5–7] hydrogen storage materials,[8,9] tissue scaffolds,[10,11] and low-dielectric constant materials for electronic packaging.[12] Porosity may lead to beneficial effects on mechanical or electrical properties, permeability, or adsorption and desorption of gases or liquids.[13] Critically important is the impact of porosity on the two physical properties of density and surface area.

There are two fundamental routes to porosity in polymers: (1) blowing by sudden gas expansion (as with polymer foams) and (2) the removal of one or more sacrificial phases. This paper utilizes the latter, which encompasses such diverse preparation techniques as the use of water-soluble salt crystals or acid-soluble silica spheres,[14,15] phase separating block copolymers where one phase can be preferentially hydrolyzed or removed through an alternative decomposition mechanism such as radiation induced degradation,[13,16,17] semicrystalline polymers gelling from solvent that are then carbonized,[18] and inverse or bicontinuous microemulsions.[19–21] Here we will be focusing on reaction-induced phase-decomposition [also called chemically-induced phase separation, or (CIPS)], excellently described by Inoue and coworkers.[22,23] and Williams et al.[24] CIPS, which proceeds over time as a result of chemical reactions, is similar to the well-established thermally-induced phase separation (TIPS), which involves manipulating temperature to lead to various morphologies. TIPS has been exploited in many different systems,[25] although perhaps the clearest example is that of block copolymers,[26] where the $\chi N(x)$ phase diagram may contain eight or more distinct phases. The χ parameter is that introduced by the Flory-Huggins relation, N is the degree of polymerization, and x is the composition. Also critical in the TIPS of block copolymers is the distinction between spinodal decomposition (SD) and nucleation and growth (NG), where the former is induced by a sudden

**Present address:* Luna Innovations Incorporated, 706 Forest St, Suite A, Charlottesville, VA 22903.

†*Present address:* US Army Research Laboratory, 4600 Deer Creek Loop, Aberdeen Proving Ground, Aberdeen, MD 21005.

Correspondence to: R. J. Klein (kleinr@lunainnovations.com) or J. L. Lenhart (joseph.lenhart1@arl.army.mil).

Journal of Applied Polymer Science, Vol. 117, 3300–3307 (2010)

large change in temperature or composition and leads to a bicontinuous network, and the latter is induced by slow changes and leads to spheroidal inclusions in a continuous matrix.[26] In CIPS, both SD and NG are accessible,[23,24,27,28] and selection between these two routes depends on three factors: diffusion to form separate phases (driven by thermodynamic incompatibility between the polymer and poragen), reaction chemistry, and reaction rate. As the chemical reaction proceeds, the polymer crosslink density and chemical functionality change, which can lead to further thermodynamic incompatibility, as well as restricting the diffusion kinetics associated with phase separation. The reaction rate impacts the rate of this changing thermodynamic behavior and the characteristic diffusion time scale. In general, as the ratio of diffusion to reaction rate increases, the likelihood of NG relative to SD increases.[20,23,26] Therefore, the phase separation mechanism in reactive systems may be viewed as a balance between diffusion of monomers or poragen molecules and the rate at which monomers or poragen molecules are bound in place.

The present paper utilizes a mixture of an epoxide, an amine, and an unreactive alcohol to produce spheroidal voids in an epoxy matrix, after removal of the alcohol which acts as a poragen. The advantages of the present technique over other methods are several-fold. First, the chemistry is limited to only three or four inexpensive chemicals, which have the benefits of being: stable relative to other reactive chemistries such as isocyanates, methacrylates, or silicones; relatively non-toxic; and very forgiving to alterations of the preparation method. Methods such as bicontinuous microemulsions or SD of block copolymers, which have the benefit of producing open pore structures that are in some cases better for membrane applications, involve expensive starting materials (tailored block copolymers) or complex formulations (oils, water, polymer starting materials, and interfacial agents[20]). Second, the pore size produced by the present CIPS method can be easily adjusted by changing reaction rate (by temperature or catalyst concentration) or concentration of unreactive alcohol, to produce spheroidal pores ranging from tens of μm to tens of nm. Third, the epoxy and amine used in this study are available in a wide range of molecular weights (by modifying the spacer length between reactive endgroups), and the spacer chemistry (propylene glycol in the current study) can be easily exchanged to induce significant changes in the mechanical and electrical properties of the final epoxy.

Ultimately, the purpose of this paper is to highlight a simple and generally applicable mechanism to control pore size (μm to tens of nm) and pore volume fraction by controlling reaction kinetics and phase behavior in a crosslinking system. While the system used in this study was an epoxy resin composed of diepoxy and diamine monomers with an alcohol poragen, the technique is applicable to a broad range of crosslinking resins, where the changes in interactions or crosslink density during cure are substantial enough to impact polymer-poragen miscibility.

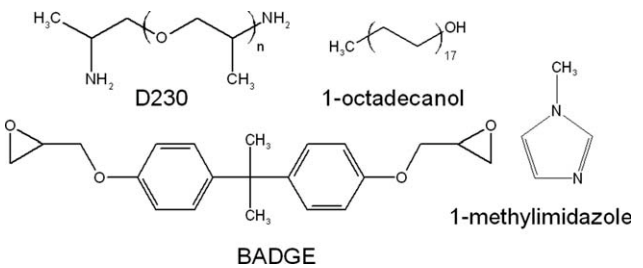

Figure 1 Structures of the BADGE (epoxide), D230 (amine crosslinker), low-molecular weight filler 1-octadecanol, and catalyst 1-methylimidazole. For the amine used here, the average molecular weight is 230 g/mol, which equates to $2 < n_{avg} < 3$.

EXPERIMENTAL

Materials

All samples utilized the same di-functional epoxide mixed in stoichiometric proportions with a tetra-functional amine. The epoxide was glycidyl end-capped poly(bisphenol A-*co*-epichlorohydrin) (BADGE), with average molecular weight 345 g/mol, obtained from Sigma-Aldrich. The amine was poly(oxypropylene)-diamine (D230), a jeffamine, with average molecular weight 230 g/mol, obtained from Sigma-Aldrich. Structures of the BADGE and D230 are shown in Figure 1. Jeffamines are commonly used in epoxy reactions, and it is expected that the method of generating porosity in this paper can be extended to other jeffamine starting materials.

1-octadecanol (95 %) was obtained from Fisher Scientific. 1-methylimidazole (99+ %), under the trade name IMICURE AMI-1 curing agent, was obtained from Air Products and Chemicals. The densities of the epoxide, amine, and octadecanol are 1.160, 0.9702, and 0.8120 g/cm^3, respectively, meaning that a sample designated 40 wt% octadecanol contains 48 vol%. This assumes additivity of volumes in the mixed state.

Sample preparation

The epoxide and amine were mixed in stoichiometric proportions with a mechanical mixer for 5 min at 1500 rpm. The octadecanol was melted in an 80-90 °C oven in predetermined masses, the epoxy liquid was preheated to 90°C, and the two liquids were mixed at ~ 90 °C for 2 min at 1200 rpm. The octadecanol, which

crystallizes at about 58°C, was processed above 70°C at all times. If needed, methylimidazole was measured (via a micropipette) and added immediately prior to the final mixing stage. Samples were cured for 15 h at the specified temperatures. They were then fractured at 0°C, and the octadecanol was removed under a 125°C vacuum for 17 h.

Characterization and image analysis

Images were taken with a Zeiss Supra55VP, field emission gun, scanning electron microscope (SEM). Samples were coated with a gold-palladium mixture and imaged with 5 kV accelerating voltage, in high vacuum mode. For most samples a secondary electron detector was used (working distance 15 mm), but in surfaces where pores were very small or not present (pore diameter < 50 nm), a shorter working distance (5 mm) and the in-lens detector were used.

Volume fractions of pores V_p were estimated using the rule of classical stereology that the average volume fraction of the species of interest is equal to the average proportion of test points that are covered by the species of interest ($V_V = P_P$).[29] A grid of 230 points was visually assessed to obtain the volume fraction of pores. An assumption was made that the fracture surface is flat, rather than three-dimensional, and the inaccuracy of this probably overestimates the pore volume fraction slightly, especially for a higher volume fraction of pores. However, the measured V_p never exceeded the maximum V_p of 48 vol%, so the overestimation is not unphysical.

The gel time is approximated as the time during the curing process at which a sharp increase in viscosity occurs that accompanies long-range network formation. Relative changes in viscosity were determined qualitatively by stirring the mixture every 30 s with a stainless steel probe inserted through a port in the curing oven.

RESULTS AND DISCUSSION

Composition plays a critical role in phase separation of this system. As composition increases from 30 wt% to 50 wt% octadecanol at a cure temperature of 90°C, the pores in Figure 2 increase from barely visible with the SEM (diameters on the order of 10 nm) to extremely large (~ 3 μm). To the naked eye, the 30 wt% sample is optically transparent whereas samples with higher octadecanol fraction are opaque and appear white.

Cure temperature is also an important variable, and delineates in rough terms the impact of cure rate. As cure temperature decreases from 90 to 75°C (micrograph (d) versus (b) in Fig. 2), pore diameter increases by a factor of ~ 2. In terms of the primary driving force impacting the gel point as the temperature is lowered, it is difficult to distinguish between thermodynamic miscibility between components and the kinetic-based time to gel. However, based on the qualitative observation that the sample at 75°C takes significantly longer to gel than a sample at 90°C, as well as the more spheroidal pore shapes in the 75°C micrograph, the time to gel is likely the predominant factor. As temperature decreases, reaction rate decreases, time to gel increases, and the components have longer times to phase separate.

The addition of methylimidazole as a catalyst can increase the cure rate substantially. The imidazole was systematically used to "quench" pores at early stages of growth, prior to extensive growth of octadecanol inclusions. The fraction of imidazole is sufficiently small in the mixtures here that it will not lead to significant shifts in composition on a thermodynamic phase diagram, so changes observed in morphology must arise from kinetically arresting the process of phase separation. While nucleophilic catalysis using imidazole derivatives in epoxy-anhydride resin systems is mechanistically easily explained via ring-opening catalysis,[30,31] it is more challenging to establish how nucleophilic catalysis accelerates the epoxy amine addition reaction. Imidazole likely catalyzes the amine-epoxide reaction by assisting the nucleophilic addition of the amine. This may occur via an intermediate imidazole-epoxy adduct, where after ring opening the approaching amine substitutes the imidazole on the epoxy carbon as shown in Figure 3. The net result is an accelerated epoxy-amine cure. The precise mechanism is unclear but there is a definite increased cure rate in the presence of the imidazole. Figures 4 and 5 denote the dramatic changes observed in the morphology as the cure rate increases: pore diameters decrease from microns to tens of nanometers until, at a critical fraction of imidazole, pores are no longer visible by SEM. Pores are clearly visible at imidazol fractions up to and including 0.6 wt%, with decreasing average pore size as the imidazol content increases. At imidazole loadings between 0.6 and 0.9 wt% only a small number of pores are identifiable, although the morphology of the fracture surface does show interesting changes. All samples with imidazole mass fraction greater than 0.9 wt% (not shown here) exhibited no visible pores, similar to Figure 5(c). The texture of the fracture surface contains different ridge structure and topological features in the higher imidazole mass fractions. This suggests that even with no visible pores in micrograph (c), there may still be stress concentrators in the form of high local concentrations of octadecanol, thereby leading to a rough surface. It should be noted that the interaction between the two concurrent processes, curing and the phase separation, may impact the molecular architecture of the crosslinked network, which

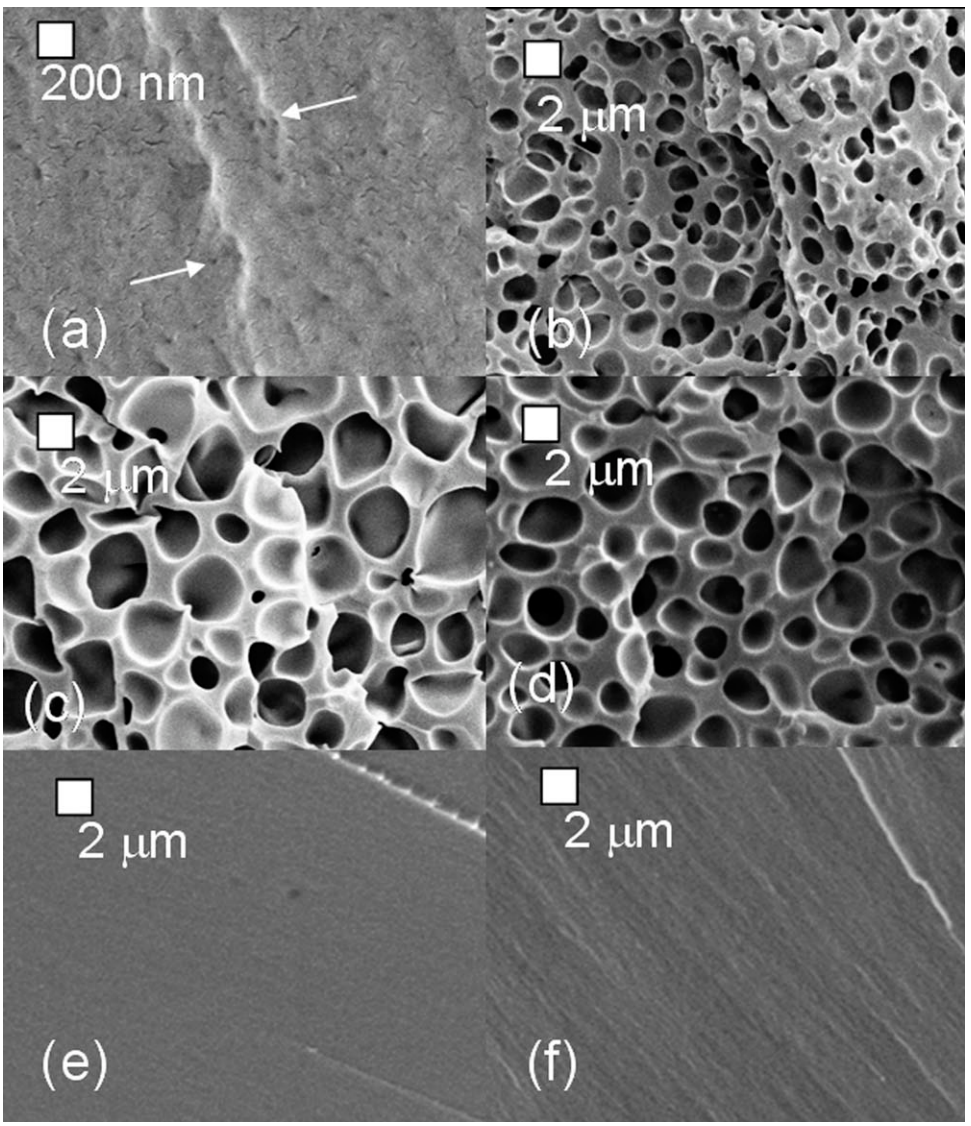

Figure 2 Epoxies cured at 90°C, where the octadecanol has been evaporated, for (a) 30 wt% octadecanol, (b) 40 wt% octadecanol, and (c) 50 wt% octadecanol. (d) epoxy cured at 75°C with 40 wt% octadecanol. Arrows indicate the location of small pores. Images (e) and (f) indicate 40 wt% octadecanol cured epoxies prior to evaporation of the octadecanol.

would also affect the mechanical and fracture behavior of the network.

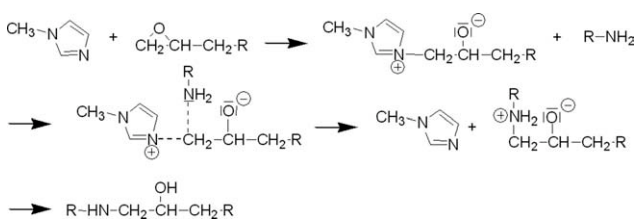

Figure 3 Schematic of a nucleophilic imidazole derivative facilitating the cure of an epoxy and amine. The imidazole opens the epoxy ring, generating a positive charge shared between the imidazole nitrogen and the adjacent epoxy carbon, which then adds to the amine. The imidazole is then regenerated to catalyze other epoxy-amine additions.

Many applications are concerned with the fraction of pores that are continuous or closed. For example, in the cases of membranes, catalysts, or sensors, a continuous porous structure could be desirable. By this method, although pores tend towards spheroidal shapes, there can still be a considerable fraction of interconnected pores. As pore diameter increases along with pore volume fraction, the connectivity between pores also increases. At high pore fractions, such as those obtained for 0.4 wt% imidazole at 90°C, $\sim$ 75% of pores are connected at least one other pore (based on image analysis). When pore diameter drops below 200 nm, the connected fraction drops below 10%. The pore connectivity can potentially be improved through various mechanisms including: increasing octadecanol volume fractions above 40 wt%; accessing bicontinuous structures that

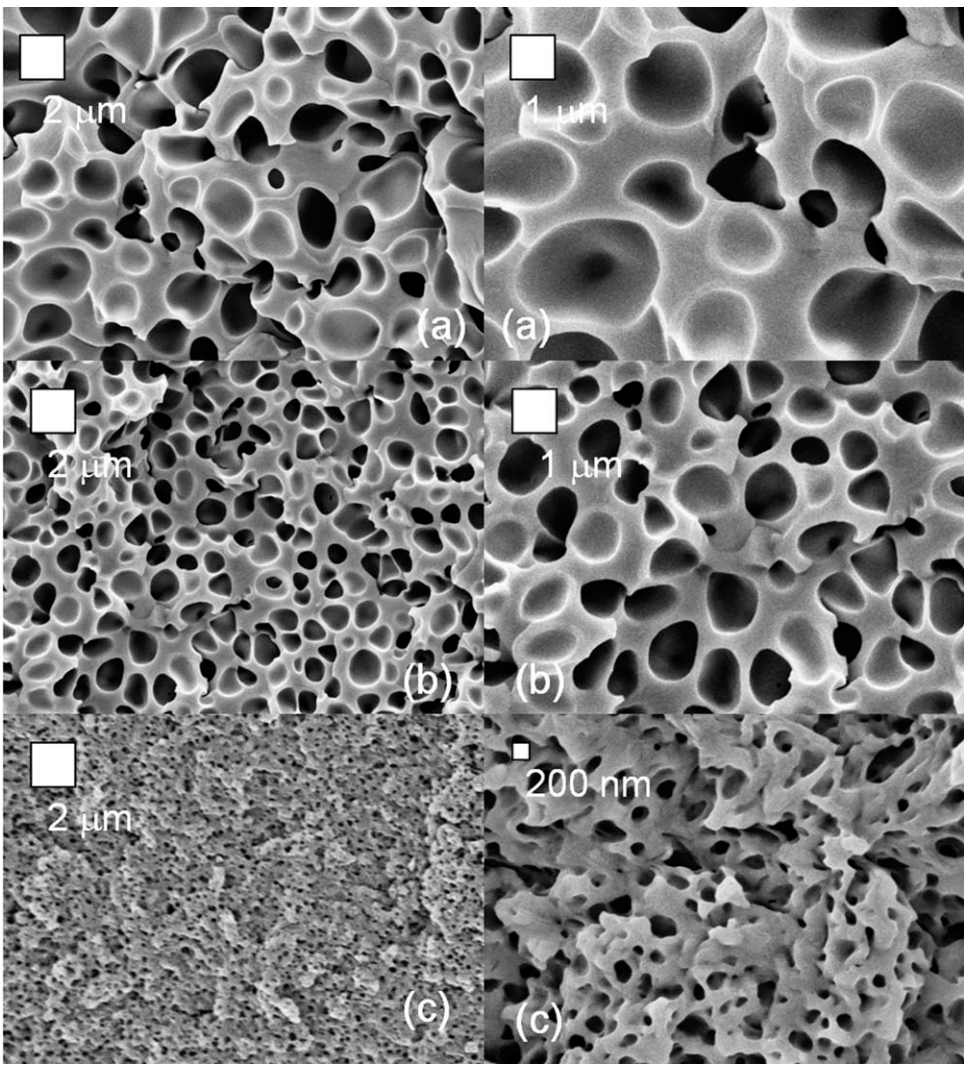

Figure 4 Fracture surfaces of epoxies cured at 90°C with 40 wt% octadecanol: (a) 0.3 wt% imidazole, (b) 0.4 wt% imidazole, and (c) 0.5 wt% imidazole. In (c), the smearing in the midsection is due to charging.

have been observed with self assembly or reactive blending methodologies[32]; or exploiting surfactants and high-internal-phase emulsions to access interconnected and self assembled structures.[33] A study of pore interconnectivity is beyond the scope of this paper, but is a primary focus of ongoing research.

Data gleaned from the SEM micrographs, for varying imidazole fraction at 40 wt% octadecanol and 90°C, are plotted in Figure 6. This plot includes the characteristic parameters of pore diameter, pore volume fraction, and gel time. The key point is that pore size is tunable across three orders of magnitude with a very simple change to the formulation, via the addition of catalyst to increase the reaction rate. Gel time decreases linearly with the addition of imidazole. A sizeable drawback to the method, however, is represented by the decrease in pore volume fraction: since the kinetics favor decreases in pore diameter rather than thermodynamics, there can be a substantial fraction of the sacrificial phase trapped in the matrix as the cure rate becomes very high, leading to a simultaneous decrease in pore volume fraction. The octadecanol is initially miscible with the epoxy matrix, and as the epoxy reacts quickly in the presence of imidazole, there is insufficient time for the octadecanol to diffuse into micron-scale phase separated regions.

Therefore, an interesting question arises when considering the decrease in pore volume fraction with increasing cure rate: after high temperature vacuum treatment, is the octadecanol that was frozen into the matrix during cure sufficiently free to diffuse out? Vacuum treatment of thin samples containing 1 wt% imidazole and 40 wt% octadecanol at 125°C for 48 h removed 80% of the octadecanol, indicating that much of the excess octadecanol is not tightly bound in the cured epoxy. The minor fraction that is not removed is due to very slow diffusion of the octadecanol in the epoxy and a small solubility of the octadecanol in the cured epoxy. Significant

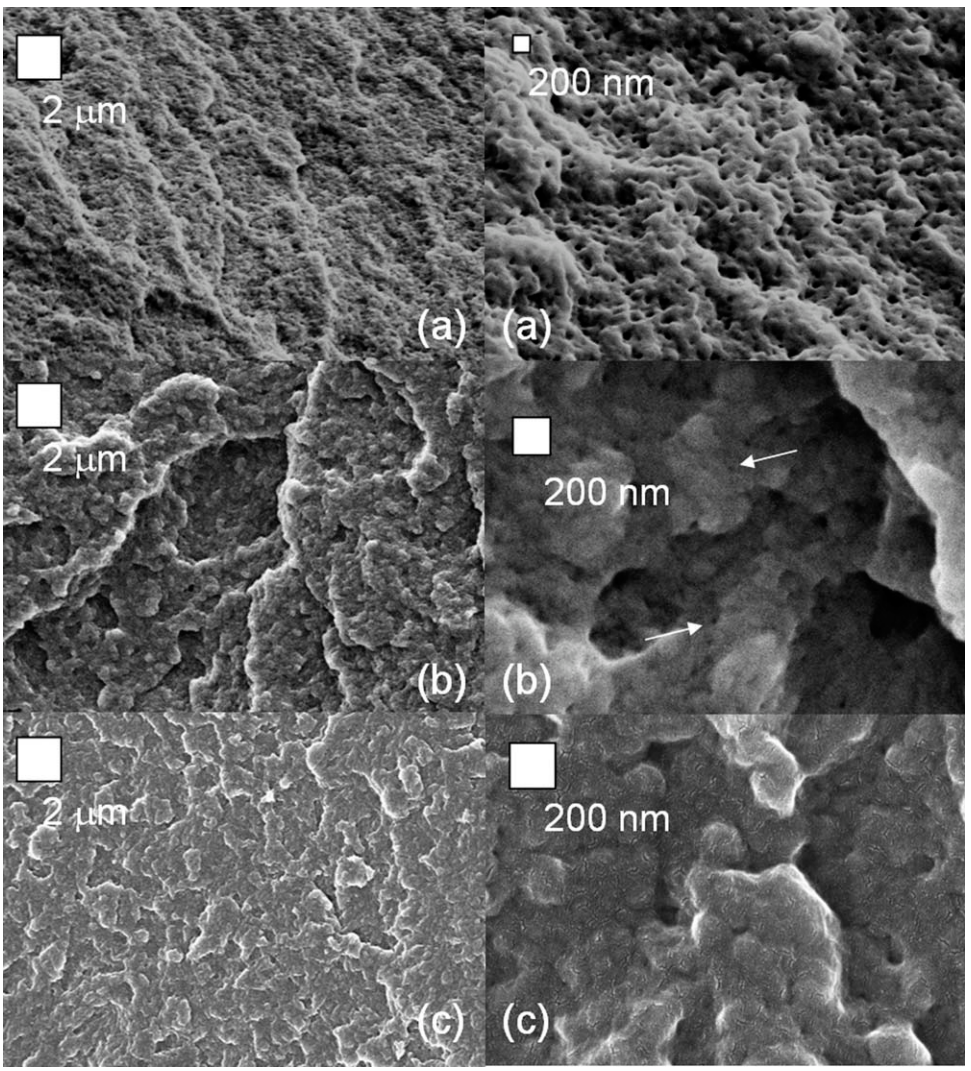

Figure 5 Fracture surfaces of epoxies cured at 90°C with 40 wt% octadecanol: (a) 0.6 wt% imidazole, (b) 0.8 wt% imidazole, and (c) 0.9 wt% imidazole. Arrows indicate the location of small pores. In the high-magnification image of (c), the "cracks" are actually due to the gold-palladium coating, and not related to the polymer fracture surface.

concurrent cracking of the matrix occurred with octadecanol removal in the samples with no visible pores, representing unsupported shrinkage: removal of the excess octadecanol must lead to collapse of the surrounding epoxy chains, since the temperature is significantly above the epoxy T_g. There is a slight decrease in the T_g in the matrix phase of these non-phase separated epoxies following octadecanol removal, which could be explained by either plasticizing of the matrix by trace octadecanol, a change in the effective network architecture (i.e., entanglements, loops, and dangling end defects), or the presence of free surfaces or pores that are not observable in the SEM.

As mentioned in the introduction, CIPS can lead to either SD or NG depending on several factors. In fact, in many of the previous CIPS studies, such as those by Gan et al.,[34] Girard-Reydet et al.,[28] Inoue and coworkers,[22,23] and Remiro et al.,[35] SD is seen at early stages of growth, and often continues to be present, leading to cocontinuous morphology even in late stages of growth. In the images obtained here, SD does not manifest at any point (as far as we could observe, there was no intermediate morphology in the transition from nano-sized pores to no pores). This occurs because of the small driving force for phase separation between octadecanol and the reacting epoxy oligomers. The former is confirmed by the high fraction of octadecanol that remains in the continuous matrix even after slow cure (10–25 % of the original amount of octadecanol). The relatively large size of the alcohol, while having a negative influence on interdiffusion rates, is shown to be a minor factor by studies that have shown high-molecular weight polymers to have the capability to phase separate into a cocontinuous morphology.[23,28,35] Note that the NG mechanism includes growth of pores both by diffusion of

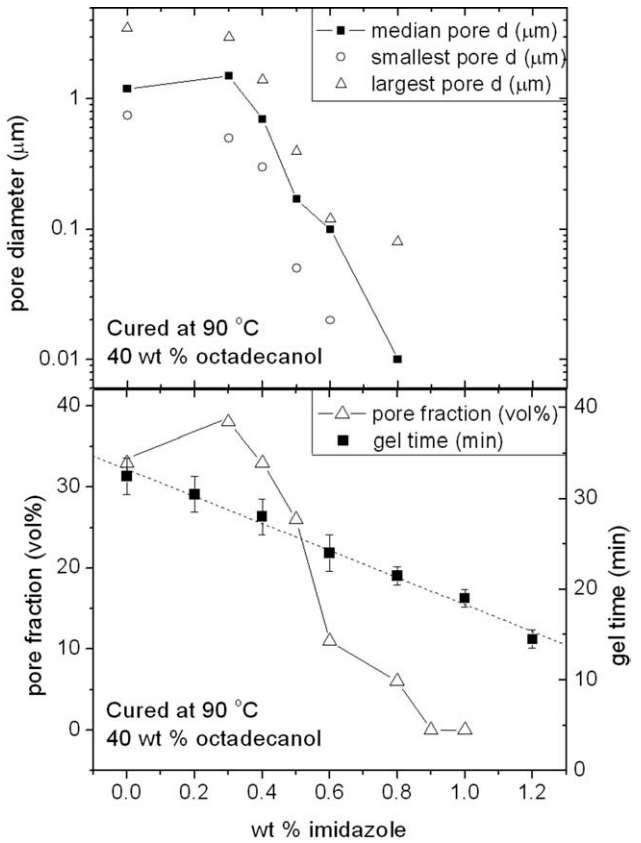

Figure 6 Pore diameter *d*, volume fraction, and gel time as a function of the amount of imidazole added relative to the amount of epoxy. All data represent a curing temperature of 90°C and 40 wt% imidazole. The dashed line is the best linear fit to the gel times and solid lines are shown to guide eyes. If not shown, estimated errors are ±10%.

material out of the matrix phase and coalescence of nearby pores.

Similar cases to the present, where NG is the only visible morphology throughout the curing process, were found by Okada et al.,[36] Kiefer et al.,[27,37] Siddhamalli et al.,[38] and Inoue.[23] Typically, NG is found in systems with low-molecular weight components as the phase separating part, such as cyclohexane by Kiefer et al.[27] or dimethylheptanone by Plummer and Keifer.[37] The formation of a cocontinuous network in the present work should be possible, based on theoretical considerations and prior experimental work, by increasing the reaction rate while simultaneously decreasing miscibility. The former can be achieved by increasing cure temperature or by using a more active catalyst (the influence of imidazole on reaction rate reaches a plateau near 2 wt%). The latter can be addressed by modifying the chemical structure of the small molecule so that the χ parameter of mixing increases. Preliminary experiments using alcohols of lower molecular weight (e.g., octanol and dodecanol) has led to increased miscibility, therefore more strongly favoring NG over SD. Oligomers or polymers of higher molecular weight may therefore be needed to achieve a cocontinuous structure.

SUMMARY

This paper has demonstrates a simple and broadly applicable method to provide precise control of polymer porosity over more than two orders of magnitude, from the micron to the nanometer scale, by controlling the crosslinking reaction rate in a phase separating system. The sacrificial phase, octadecanol, is removed by vacuum-assisted evaporation once the epoxy components have reacted to form a solid, porous matrix. The pore diameter is controlled through variations in cure temperature and addition of the catalyst methylimidazole. While this system was composed of an epoxy matrix and an alcohol poragen, the technique is applicable to other resin chemistries, once the impact of polymer-poragen compatibility, diffusion kinetics, and reaction kinetics are fully understood.

As cure temperature decreases, pore diameter increases, likely due to an increase in the cure time (although it is difficult to rule out the additional impact of cure temperature on phase separation thermodynamics). The longer the cure time, the more time there is for the chemical components to fully diffuse into separate phases. The addition of the catalyst has a similar impact: a decrease in the cure time promotes smaller pores by quenching the phase separation in early stages. Most of the excess (nonphase separated) octadecanol can be removed by prolonged heating under vacuum. Cure time decreases linearly with imidazole fraction. Only NG, not SD, was observed as a phase separation mechanism in this system.

The method of chemically-induced phase-separation has been demonstrated by previous investigations. However, the importance of the present approach hinges on the simplicity of the chemical formulation, the ease by which other resin chemistries can be substituted, and the precise control of pore size down to the nanometer scale by the addition of a small amount of catalyst. Future work will focus on controlling pore connectivity and shape as well as incorporating particulate fillers to modify the properties of the porous material.

The authors thank Bonnie McKenzie at Sandia National Laboratories for excellent SEM images. The bulk of this work was completed at Sandia National Laboratories, and further research is progressing at the U.S. Army Research Laboratory by JLL. Sandia is a multiprogram laboratory operated by Sandia Corporation, a Lockheed Martin Company, for the United States Department of Energy's National Nuclear Security Administration under contract DE-AC04-94AL85000. Certain commercial equipment and materials are identified in this article to specify adequately the experimental

procedure. In no case does such identification imply recommendations by the Army Research Laboratory nor does it imply that the material or equipment identified is necessarily the best available for this purpose.

References

1. Rolison, D. R. Science 2003, 299, 1698.
2. Adhikari, B.; Majumdar, S. Prog in Polym Sci 2004, 29, 699.
3. Potyrailo, R. A. Angew Chem Int Ed Engl 2006, 45, 702.
4. Orellana, G.; Moreno-Bondi, M. C., Eds. Frontiers in Chemical Sensors, Springer-Verlag: New York, 2005.
5. Xu, K. Chem Rev 2004, 104, 4303.
6. Whittingham, M. S. MRS Bull 2008, 33, 411.
7. Long, J. W.; Dunn, B.; Rolison, D. R.; White, H. S. Chem Rev 2004, 104, 4463.
8. Zuttel, A.; Orimo, S. MRS Bull 2002, 27, 705.
9. Powell, G. L. J Alloys Compd 2007, 446, 402.
10. Freed, L. E.; Vunjaknovakovic, G.; Biron, R. J.; Eagles, D. B.; Lesnoy, D. C.; Barlow, S. K.; Langer, R. Biotechnology 1994, 12, 689.
11. Levesque, S. G.; Lim, R. M.; Shoichet, M. S. Biomaterials 2005, 26, 7436.
12. Jain, A.; Rogojevic, S.; Ponoth, S.; Agarwal, N.; Matthew, I.; Gill, W. N.; Persans, P.; Tomozawa, M.; Plawsky, J. L.; Simonyi, E. Thin Solid Films 2001, 398, 513.
13. Aubert, J. H.; Sylwester, A. P. Mater Technol 1994, 9, 4.
14. De Groot, J. H.; Nijenhuis, A. J.; Bruin, P.; Pennings, A. J.; Veth, R. P. H.; Klompmaker, J.; Jansen, H. W. B. Colloid Polym Sci 1990, 268, 1073.
15. Jiang, P.; Hwang, K. S.; Mittleman, D. M.; Bertone, J. F.; Colvin, V. L. J Am Chem Soc 1999, 121, 11630.
16. Li, S.; Garreau, H.; Vert, M.; Petrova, T.; Manolova, N.; Rashkov, I. J Appl Polym Sci 1998, 68, 989.
17. Durkee, D. A.; Gomez, E. D.; Ellsworth, M. W.; Bell, A. T.; Balsara, N. P. Macromolecules 2007, 40, 5103.
18. Lagasse, R. R.; Schroeder, J. L. In Materials Research Society Symposium Proceedings: Advances in Porous Materials, Komarneni, S., Smith, D. M., Beck, J. S., Eds.; Materials Research Society: Boston, 1994.
19. Liu, J.; Gan, L. M.; Chew, C. H.; Teo, W. K.; Gan, L. H. Langmuir 1997, 13, 6421.
20. Candau, F.; Pabon, M.; Anquetil, J.-Y. Colloids Surf A Physicochem Eng Asp 1999, 153, 47.
21. Yong, C. P.; Gan, L. M. Polymer Particles; Springer: Berlin, 2005.
22. Kim, B. S.; Chiba, T.; Inoue, T. Polymer 1993, 34, 2809.
23. Inoue, T. Prog Polym Sci 1995, 20, 119.
24. Williams, R. J. J.; Rozenberg, B. A.; Pascault, J. P. Adv Polym Sci 1997, 128, 95.
25. Whinnery, L. L.; Even, W. R.; Beach, J. V.; Loy, D. A. J Polym Sci Part A: Polym Chem 1996, 34, 1623.
26. Bates, F. S. Science 1991, 251, 898.
27. Kiefer, J.; Hilborn, J. G.; Manson, J. A. E.; Leterrier, Y.; Hedrick, J. L. Macromolecules 1996, 29, 4158.
28. Girard-Reydet, E.; Sautereau, H.; Pascault, J. P.; Keates, P.; Navard, P.; Thollet, G.; Vigier, G. Polymer 1998, 39, 2269.
29. Baddeley, A.; Jensen, E. B. V. Stereology for Statisticians; Chapman and Hall/CRC: New York, 2005.
30. Dearlove, T. J. J Appl Polym Sci 1970, 14, 1615.
31. Rocks, J.; Rintoul, L.; Vohwinkel, F.; George, G. Polymer 2004, 45, 6799.
32. Pernot, H.; Baumert, M.; Court, F.; Leibler, L. Nat Mater 2002, 54, 1.
33. Brinker, C. J.; Lu, Y.; Sellinger, A.; Honyou, F. Adv Mater 1999, 11, 579.
34. Gan, W.; Yu, Y.; Wang, M.; Tao, Q.; Li, S. Macromol Rapid Commun 2003, 24, 952.
35. Remiro, P. M.; Marieta, C.; Riccardi, C. C.; Mondragon, I. Polymer 2001, 42, 09909.
36. Okada, M.; Inoue, G.; Ikegami, T.; Kimura, K.; Furukawa, H. Polymer 2004, 45, 4315.
37. Plummer, C. J. G.; Kiefer, J. Colloid Polym Sci 2000, 278, 736.
38. Siddhamalli, S. K.; Kyu, T. J Appl Polym Sci 2000, 77, 1257.